Evolution of Electron Hole and Electron Wave Pulses in a Single-Ended Magnetoplasma

doi: 10.1063/1.865745

Evolution of electron hole and electron wave pulses in a single-ended magnetoplasma

S. Iizuka and H. Tanaca
Faculty of Engineering, Yokohama National University, Yokohama 240, Japan

(Received 18 April 1986; accepted 3 September 1986)

Formation and propagation of the electron phase-space hole and electron wave pulse (Trivelpiece–Gould mode) are experimentally investigated in a single-ended plasma in the very first stage of double layer formation. As soon as the rarefaction pulse excited at a collector terminating the plasma arrives at a plasma source, the electron holes are formed and propagate toward the collector with a speed comparable to the electron thermal speed. The electron energy distribution function dips at the hole and becomes broader in the upper stream region of hole propagation. The compression pulse formed in front of the plasma source just after rarefaction pulse arrival does not have a direct effect on the hole excitation.

I. INTRODUCTION

Recently, formation of the electron phase-space hole has attracted attention in relation to strong double layer formation.[1] The hole[2] evolves as a stationary BGK mode[3] consisting of trapped electrons in a narrow positive potential spike. In computer simulations[4,5] such a hole generation is observed just before the double layer formation when a potential difference is applied between two plasma sources (this configuration corresponds to the double-ended Q-machine). The hole generated at the low potential plasma source propagates toward the higher potential side with a speed on the order of the electron thermal speed. The same situation is also observed when the high potential plasma source is replaced by a simple collector boundary[6] (this configuration corresponds to the single-ended Q-machine). In this case, the plasma comes from a grounded single plasma source that emits electrons and ions with fixed velocity distribution functions and the other end of the plasma is terminated by a collector whose potential can be varied externally. When positive step voltage is applied to the collector, the plasma potential is forced to increase, resulting in a hole formation in front of the plasma source.

Experimentally, however, there has been no indication of the holes, but electron waves appear in the initial stage of the potential application to the end-collector plate in the previous single-ended Q-machine plasmas.[7–9] On the other hand, although an experiment on hole excitation has been carried out in a single-ended Q-machine plasma confined in a cylindrical wave guide, the relationship to double layer formation was not investigated explicitly.[10] However, it was found that the holes are excited effectively provided that the applied voltage exceeds a critical value of $V_{cri} \cong (m_e/2e)(\omega_{pe}a/2.4)^2$ and that the rise time of the applied voltage is on the order of $2\pi/\omega_{pe}$, where ω_{pe} is the electron plasma frequency, a is the plasma radius, and m_e is the electron mass. When the plasma density is $n_0 \cong 5\times10^9$ cm^{-3} and $a = 1.3$ cm, for example,[7] $V_{cri} \cong 1.3$ kV, which was much higher than the applied collector voltage V_c (< 100 V). Therefore, only the electron wave excitation was expected in that case. However, since $V_{cri} \cong 2$ V in our experiment, we can easily excite the holes even in the lower voltage regime of $V_c \lesssim 17$ V, if a step voltage with short rise time is applied.

The object of this paper is to report the first experiment of the hole evolution in the initial stage of double layer formation when a step voltage is applied to the collector in the single-ended plasma emitter device. As briefly reported previously,[11] excitation of the electron holes is triggered by the electron waves (Trivelpiece–Gould mode).

In Sec. II the experimental results are presented. Discussions and conclusions are described in Secs. III and IV, respectively.

II. EXPERIMENTAL RESULTS

The experiment is carried out in a single-ended plasma emitter device shown in Fig. 1. The plasma emitter used here produces a plasma by synthesizing electrons and ions emitted thermionically from barium oxide and potassium water glass (K_2SiO_3), respectively. The construction and operation are briefly described in Ref. 12. A potassium ion plasma, produced by a 3 cm diam plasma emitter placed at $z = 0$, flows along the homogeneous magnetic field B_0 and is terminated by a 3 cm diam cold collector plate placed at $z = L$. The whole plasma column is surrounded by a grounded metal cylinder of radius $b = 3$ cm. The potential of the plasma emitter is always at the ground level.

First, a positive step voltage is applied to the collector at $t = 0$. Then, signals in the plasma are detected by an axially movable probe made of 2 mm × 2 mm metal plate and even-

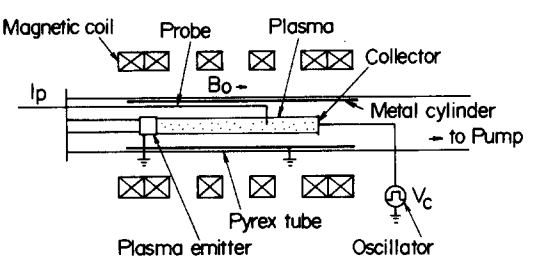

FIG. 1. Experimental apparatus. The plasma emitter produces a potassium ion plasma by synthesizing electrons and ions emitted thermionically from barium oxide and potassium water glass, respectively.

 0031-9171/86/124035-05$01.90

tually recorded by an x-y recorder through a box-car integrater. (We carried out similar measurements by using a 0.1 mm diam and 5 mm long wire probe and obtained the same results.) In the normal experiment the length of the plasma column is $L = 60$ cm, the applied collector voltage is $V_c = 5$–17 V, and the magnetic field is $B_0 = 1.5$ kG. The electron density and temperature are $n_0 = 10^6$–10^7 cm^{-3} and $T_e \cong 0.2$ eV, respectively.

Figure 2 shows a temporal variation of the electron saturation current signal I_p of the probe when the step voltage V_c, changing from 0 to 15 V with rise time of $\lesssim 0.1$ μsec, is applied to the collector at $t = 0$. Here, we clearly find an evolution of large amplitude current oscillation after $t = 0$, as is often seen on the single-ended device with a positively biased collector plate.[13] Recently, it was shown that this oscillation is related to a dynamic behavior of a moving double layer.[14] The first period $t = 0 - 210$ μsec corresponds to a time phase where the double layer moves from the source to the collector with a speed of $\sim 3C_s$, where C_s is the ion acoustic speed. Similar large amplitude oscillations accompanied by a moving double layer were found in computer simulations.[4,6] Here we examine the details of the plasma response in the initial stage of the double layer formation shown by the arrows in Fig. 2.

Figure 3(a) shows the signals I_p with the probe position z as a parameter. Just after $t = 0$ we find that a rarefaction pulse is generated at the collector and propagates toward the emitter. When the pulse arrives at the emitter, a compression pulse is formed there and propagates back toward the collector. Then, after the reflection the compression pulse propagates again toward the emitter. The speeds of the rarefaction v_R and compression v_C pulses, i.e., $v_R \cong v_C \cong (6-7)\times 10^7$ cm/sec, are faster than the electron thermal speed $v_{Te} \cong 2\times 10^7$ cm/sec.

On the other hand, we observe the generation of another pulse at the emitter just after arrival of the rarefaction pulse. It is a negatively perturbed density pulse moving with a speed $v_H \cong 6.7\times 10^6$ cm/sec, on the order of the electron thermal speed, which might suffer a strong electron Landau damping. However, since it does not change much in shape, we think that this slow pulse should be an electron hole pulse. Propagations of these pulses are plotted in a z–t diagram as shown in Fig. 3(b), where open and closed circles correspond to the centers of the rarefaction and compression pulses, respectively, and the dotted circles to the electron

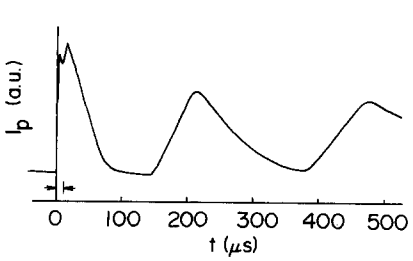

FIG. 2. Temporal evolution of the probe current I_p after the application of step voltage $V_c = 15$ V to the collector at $t = 0$. Detailed measurements are made in the time interval shown by the arrow.

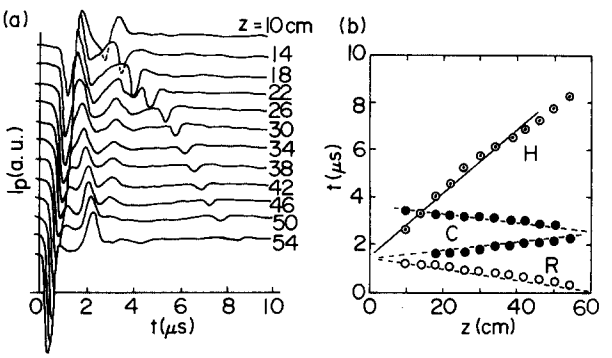

FIG. 3. Temporal and spatial evolutions of the probe current. (a) Probe signals I_p at different positions z. (b) Propagating traces of the centers of rarefaction R (○), compression C (●), and hole H (⊙) pulses. Here $V_c = 15$ V and $n_0 \cong 3\times 10^6$ cm^{-3}. Solid and dotted lines show the averaged traces of the pulses.

hole pulse. It appears from this figure that the arrival of the rarefaction pulse at the emitter gives a key triggering effect for the excitations of both the hole and compression pulses.

To confirm that the slow pulse is actually an electron hole, measurement of the electron energy distribution function is necessary. Figure 4(a) shows the probe signals I_p detected at $z = 6$, 8, and 10 cm. The R and H indicate the rarefaction and hole pulses, respectively. The energy distribution function around the pulse H is measured by an electrostatic energy analyzer consisting of a first grounded grid, a second control grid, and a positively biased end plate. Figure 4(b) shows the end plate current I_E as a function of the control grid voltage V_G at a fixed sampling time of a box-car integrater as shown on the top trace in Fig. 4(a). At this sampling time the center of the hole should be at $z = 8$ cm. A characteristic I_E-V_G curve is obtained with a beam-like structure, especially in the analyzer position $z = 7$–9 cm.

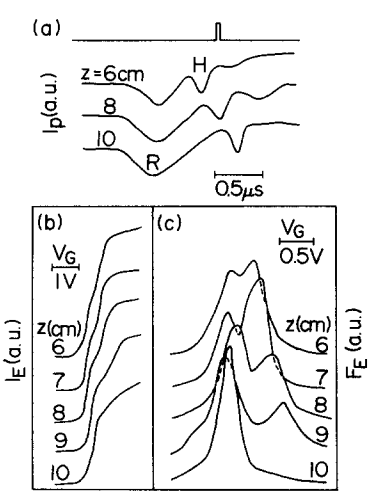

FIG. 4. Measurements of the electron energy distribution functions in the hole region. (a) Probe signal I_p. Here R and H indicate rarefaction and hole pulses, respectively. (b) The $I_E - V_G$ curve of energy analyzer and (c) energy distribution function $F_E(V_G)$ obtained from $\partial I_E/\partial V_G$. These data are measured at a sampling time shown on the top trace in (a).

The structure is again clearly confirmed by differentiating the curve against V_G, which gives an energy distribution function $F_E(V_G)$ (obtained from $\partial I_E/\partial V_G$) as shown in Fig. 4(c). A double hump profile in $F_E(V_G)$ is observed at the hole region $z = 7$–9 cm. Therefore the slowly propagating pulse H in Fig. 3 really has a hole structure in the energy distribution function, i.e., the electron hole. It is noted that the half-width of the distribution function becomes broader in the upper-stream region ($z < 10$ cm) of the hole propagation. This tendency is also found in Fig. 12 of the simulation of Ref. 5.

The speed, width, and amplitude of the hole depend on the collector voltage V_c as shown in Fig. 5. Here, $\tilde{I}_p$ means the amplitude of the negatively perturbed electron saturation current at the hole center, and $M = v_H/v_{Te}$ is the hole Mach number normalized to the electron thermal speed. The half-width δ of the hole is estimated from the supposed relation $\delta = v_H \tau$, where τ is the half-time width of the pulse. We see that all values increase with the voltage V_c. That is, the larger the hole amplitude, the faster the hole speed and the wider the hole width, being quite different from the properties of the usual solitary waves. It should also be noted that the hole speed is less than v_{Te} and the hole width δ is on the order of ten times as large as the Debye length $\lambda_D \cong 0.2$ cm.

In the case of larger voltage V_c or higher density n_0 we find not only one hole but also more than two holes as shown in Fig. 6(a). Just after $t = 0$ we find the rarefaction pulse as in the previous case, propagating toward the emitter with a speed much faster than the thermal speed. The generation of the compression pulse does not appear clearly in this case. The pulse propagations are again plotted in the z–t diagram in Fig. 6(b), where we observe several slow hole pulses besides the fast pulse. Extrapolating the pulse traces toward the emitter, these holes seem to be generated simultaneously just when the rarefaction pulse arrives at the emitter. Therefore, the rarefaction pulse rather than the compression pulse plays a decisive role on generation of the holes. The conditions for exciting many holes are rather complicated and depend on both the density n_0 and the voltage V_c.

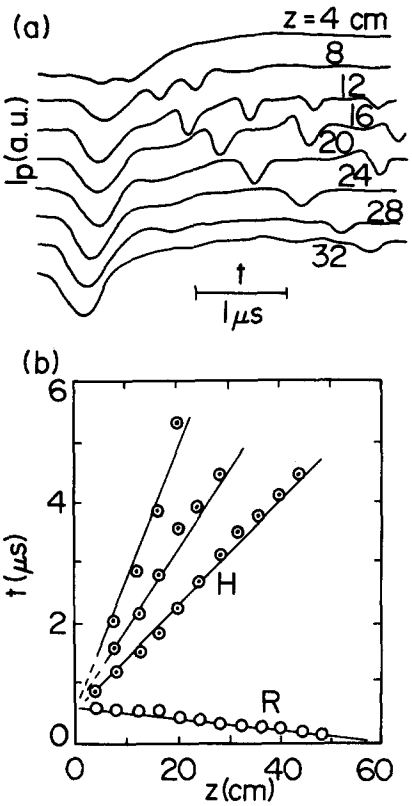

FIG. 6. Temporal and spatial evolutions of the probe current. (a) Probe signals I_p at different positions z. (b) Propagating traces of the centers of rarefaction R (○) and hole H (◎) pulses. Solid lines show the averaged traces of the pulses. Here $V_c = 16$ V and $n_0 \cong 5 \times 10^6$ cm^{-3}.

III. DISCUSSION

In order to identify the fast pulse we calculate the dispersion relation of the electron wave in a strongly magnetized plasma of radius a surrounded by a metal cylinder of radius b. Starting from the basic equations for electrons,

$$m_e\left(\frac{\partial v_e}{\partial t} + v_e \cdot \nabla v_e\right) = -e(-\nabla\phi + v_e \times B_0) - \frac{\nabla P}{n_e},$$

$$\frac{\partial n_e}{\partial t} + \nabla \cdot (n_e v_e) = 0, \quad -\nabla^2\phi = \frac{e(n_0 - n_e)}{\epsilon_0}, \qquad (1)$$

we obtain the dispersion relation of the Trivelpiece–Gould mode,[15] where $n_0 = n_i$ is the ion density, $P = 3n_e T_e$ is the electron pressure, and

$$TJ_0(Ta)/J_0(Ta) = k\,[K_0(\alpha X)I_0'(X) - I_0(\alpha X)K_0'(X)]/$$
$$[K_0(\alpha X)I_0(X) - I_0(\alpha X)K_0(X)], \qquad (2)$$

where $T^2 = k^2[-1 + 1/(\Omega^2 - 3X^2/\beta^2)]$, $\alpha = b/a$, $\beta = k_D a, X = ka, \Omega = \omega/\omega_{pe}$. Here k is the axial wavenumber, k_D is the Debye wavenumber, ω_{pe} is the electron-plasma frequency, J_0 and I_0, K_0 are the Bessel function and the modified Bessel functions, respectively, and I_0' and K_0' are differentials. Here, we adopt the following boundary conditions for the potential perturbation inside the plasma $\tilde{\phi}_p$ and in the vacuum $\tilde{\phi}_v$, i.e., $\tilde{\phi}_p(a) = \tilde{\phi}_v(a)$, $\partial\tilde{\phi}_p(a)/\partial r = \partial\tilde{\phi}_v(a)/\partial r$, and $\tilde{\phi}_v(b) = 0$.

The solid curve in Fig. 7 shows a typical dispersion relation obtained from Eq. (2) for our experimental conditions,

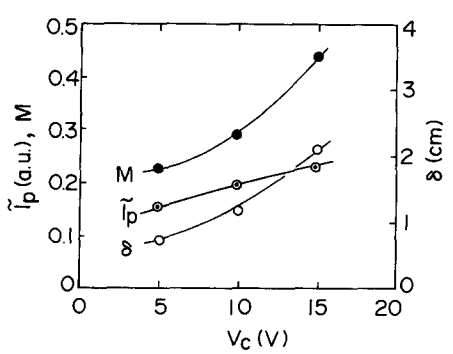

FIG. 5. Amplitude $\tilde{I}_p$ (◎), speed M ($= v_H/v_{Te}$) (●), and width δ (○) of the hole as a function of V_c. Solid curves show the tendencies of the data.

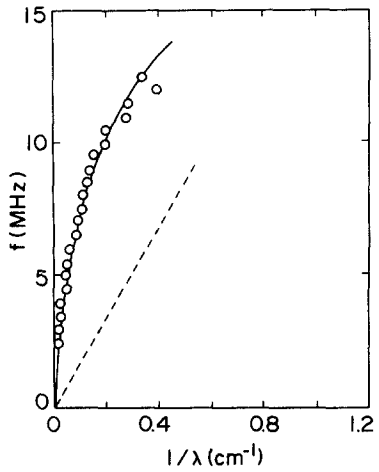

FIG. 7. Dispersion relation of Trivelpiece–Gould mode. The solid curve is obtained theoretically, and open circles show experimental data. The broken line corresponds to the electron thermal speed.

i.e., $\alpha = 3$ and $\beta = 10$. The open circles plotted are experimental data obtained by applying a sine-voltage V_c to the collector plate. We measure the wavelength λ as a function of the exciting frequency f, in good agreement with the dispersion relation. We see that the phase speed of the electron wave is $v_{TG} = (7-8)\times 10^7$ cm/sec, agreeing well with the rarefaction v_R and compression v_C pulse speeds. Therefore, the fast pulse in Fig. 3 should be the electron wave pulse. Here, we give the electron thermal speed as a broken line. Since the speed of the slow hole pulse is $v_H \lesssim v_{Te}$, the hole is on an intrinsically different branch from that of the electron wave.

In order to clarify the hole profile we calculate the Sagdeev potential $V(\Phi)$ from the Poisson equation by assuming the distribution functions for passing F_p and trapped F_t electrons. Thus

$$-V(\Phi) = \frac{K_\perp^2 \Phi^2}{2} + \int_0^\Phi d\Phi \int_{-\infty}^{\infty} du\, F(u,\Phi) - \frac{\Phi}{\gamma}, \tag{3}$$

where

$$F(u,\Phi) = F_p + F_t,$$

$$F_p = (\gamma\sqrt{2\pi})^{-1} \exp\{-[\pm(u^2 - 2\gamma\Phi)^{1/2} + M]^2/2\}$$

$$(+; u \gtrsim \sqrt{2\gamma\Phi})$$

$$(-; u \lesssim \sqrt{2\gamma\Phi}),$$

$$F_t = (\gamma\sqrt{2\pi})^{-1} \exp\{-[M^2 + \epsilon(u^2 - 2\gamma\Phi)]/2\}$$

$$(|u| < \sqrt{2\gamma\Phi}),$$

$$\gamma = \frac{\int_0^a dr\, r J_0^3(k_\perp r)}{\int_0^a dr\, r J_0^2(k_\perp r)}.$$

When $\epsilon < 0$, the distribution function F_t represents a hole. The values u, Φ, and $K_\perp$ are normalized to v_{Te}, T_e/e, and k_D, respectively. From $V(\Phi_0) = 0$ the amplitude of the hole Φ_0 is determined. Then we can get a half-width D of the hole from

$$D = \frac{\delta}{\lambda_D} = 2\int_{\Phi_0}^{\Phi_0/2} \frac{d\Phi}{\sqrt{-2V(\Phi)}}. \tag{4}$$

Figure 8 shows typical variations of Φ_0 and D as a function of η, which is introduced as a measure of the trapped electron ratio at the hole center, i.e.,

$$\eta = \frac{\int_{-\sqrt{2\gamma\Phi_0}}^{\sqrt{2\gamma\Phi_0}} du\, F_t}{\int_{-\infty}^{\infty} du\, F(u,\Phi_0)}. \tag{5}$$

It appears that the strong hole of $\Phi_0 > 1$ is formed for $\eta \gtrsim 0.5$. In our experiment we cannot exactly distinguish the distribution function of the trapped electrons from that of the passing electrons, because the profile $F_E(V_G)$ in Fig. 4(c) is perturbed in the hole region. From a rough estimation, however, we find that η may be around the value of 0.5. Furthermore, the amplitude observed in Fig. 4(c) is $\Phi_0 = e\phi_0/T_e \cong 0.5$ eV/0.2 eV $\cong 2.5$, the half-width $D = \delta/\lambda_D \cong (1.5\text{ cm} - 2\text{ cm})/0.2\text{ cm} \cong 8 - 10$, and the Mach number $M \lesssim 1$, which is consistent with the numerical results. Here, the hole amplitude $\phi_0 \cong 0.5$ V is also quite reasonable even in comparison with the other experiment.[10] Again in Fig. 8 both the speed and width increase as the amplitude increases at a fixed value of η, which qualitatively corresponds to the data in Fig. 5.

As a formation mechanism of the holes the electron–electron two-stream instability is considered.[2] For this instability the potential variation in front of the emitter is important, and it is closely related to the arrival of the rarefaction pulse as shown in Fig. 3. According to a one-dimensional simulation with $k_\perp = 0$,[6] the plasma potential in front of the emitter is immediately increased by the potential application at $t = 0$. However, in the actual plasma with a radial boundary ($k_\perp \neq 0$), the penetration speed of the collector potential

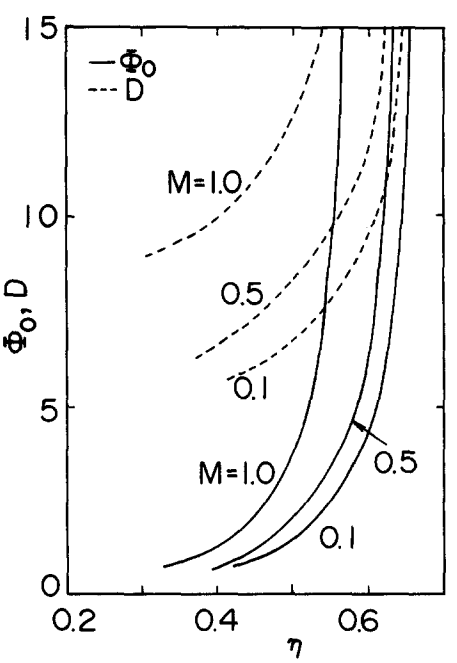

FIG. 8. Amplitude Φ_0 and width D of the holes as a function of the trapped electron ratio η with hole speed M as a parameter. Here $K_\perp = 0.2$.

toward the emitter, appearing as a wave pulse propagation, is suppressed by the shielding effect of the radial boundary, allowing only a speed of the order of the Trivelpiece–Gould mode v_{TG} ($\cong \omega_{pe}/k_\perp$). Therefore it takes a longer time for the potential variation to appear in front of the emitter, i.e., $\tau_0 \cong k_\perp L/\omega_{pe}$. This pulse should be rarefactional, as in the experiment, because it is excited at the collector by a sudden subtraction of electrons in front of the collector. Since the rarefaction pulse has a positive potential shape propagating with a speed much faster than v_{Te}, most bulk electrons cannot follow such a rapid potential increase, forming high potential plasma electrons caused by an adiabatic trapping. When the pulse arrives at the emitter, the potential in front of the emitter is forced to increase, giving rise to abrupt electron injection from the emitter into the high potential bulk plasma. Then, the hole evolves nonlinearly through the two-stream instability, accompanied by excitation of a compression pulse because of the abrupt injection. This scenario for the hole and electron wave excitations is well simulated by a computer using a particle model.[11,16] The wave reflection at the emitting boundary, i.e., at the plasma source, may be quite different from that at the nonemitting boundary.[17]

Here we note that even if the hole evolves near the emitter, it will be quite unlikely that the hole can immediately satisfy the stationary solutions shown in Fig. 8. An excess of trapped electrons would be detrapped, causing a disintegration of the hole into many small holes. Also, continuous electron injection at the emitter would excite the holes successively. The multiple holes in Fig. 6 may be generated through such processes. In addition, the detrapping and the energy dissipation of injected electrons give rise to energetic electrons in the plasma, which might be responsible for the broadening of the distribution function in Fig. 4(c). The multiple hole formation is also seen in the larger exciting voltage regime in computer simulations.[11,18]

IV. CONCLUSIONS

The detailed measurements are carried out in the initial stage of the double layer formation, where the electron hole pulses evolve just after the potential application to the collector, together with the rarefaction and compression pulses of the Trivelpiece–Gould mode. The rarefaction pulse plays an important role for exciting the hole and the compression pulses.

A hole structure observed in the electron energy distribution function agrees well with the theoretical predictions and simulations. Although no clear change occurs in the energy distribution function during the electron wave propagation, a broadening is observed in the upper stream region of the hole propagation. Therefore an effective electron heating may be expected through a process including dissipation of the injected beam as well as formation and disruption of the electron holes.

ACKNOWLEDGMENTS

The authors wish to thank Professor N. Sato for his continuous encouragement. They are also indebted to I. Hikima for his computational assistance.

The work is partially supported by a Grant-in-Aid for Scientific Research from the Ministry of Education, Japan.

[1] G. Joyce and R. F. Hubbard, J. Plasma Phys. **20**, 391 (1978).
[2] H. L. Berk, C. E. Nielsen, and K. V. Roberts, Phys. Fluids **13**, 980 (1970).
[3] I. B. Bernstein, J. M. Greene, and M. D. Kruskal, Phys. Rev. **108**, 546 (1957).
[4] N. Singh, Plasma Phys. **24**, 639 (1982).
[5] N. Singh and R. W. Schunk, Plasma Phys. Controlled Fusion **26**, 859 (1984).
[6] S. Iizuka and H. Tanaca, J. Plasma Phys. **33**, 29 (1985).
[7] W. H. M. Clark and S. M. Hamberger, Plasma Phys. **21**, 943 (1979).
[8] J. P. Hauck, N. Rynn, and G. Benford, Phys. Fluids **16**, 1946 (1973).
[9] R. Schrittwieser and J. J. Rasmussen, Phys. Fluids **25**, 48 (1982).
[10] K. Saeki, P. Michelsen, H. L. Pécseli, and J. J. Rasmussen, Phys. Rev. Lett. **42**, 501 (1979).
[11] S. Iizuka and H. Tanaca, Phys. Lett. A **103**, 57 (1984).
[12] S. Iizuka and H. Tanaca, Plasma Phys. Controlled Fusion **27**, 133 (1985).
[13] N. Sato, G. Popa, E. Märk, E. Mravlag, and R. Schrittwieser, Phys. Fluids **19**, 70 (1976).
[14] S. Iizuka, P. Michelsen, J. J. Rasmussen, R. Schrittwieser, R. Hatakeyama, K. Saeki, and N. Sato, Phys. Rev. Lett. **48**, 145 (1982).
[15] A. W. Trivelpiece and R. W. Gould, J. Appl. Phys. **30**, 1784 (1959).
[16] S. Iizuka and H. Tanaca, J. Plasma Phys. (in press).
[17] I. Ibrahim and H. H. Keuhl, Phys. Fluids **27**, 962 (1984).
[18] J. P. Lynov, P. Michelsen, H. L. Pécseli, and J. J. Rasmussen, Phys. Scr. **20**, 328 (1979).